

# Kagome lattice antiferromagnets and Dzyaloshinsky-Moriya interactions

Marcos Rigol

*Department of Physics and Astronomy, University of Southern California, Los Angeles, California 90089, USA*

Rajiv R. P. Singh

*Department of Physics, University of California, Davis, California 95616, USA*

(Dated: November 2, 2018)

We study the consequences of in-plane ( $D_p$ ) and out-of-plane ( $D_z$ ) Dzyaloshinsky-Moriya (DM) interactions on the thermodynamic properties of spin- $\frac{1}{2}$  Heisenberg model on the kagome lattice using numerical linked cluster expansions and exact diagonalization, and contrast them with those of other perturbations such as exchange anisotropy and dilution. We find that different combinations of the DM anisotropies lead to a wide variety of thermodynamic behavior, which are quite distinct from those of most other perturbations. We argue that the sudden upturn seen experimentally in the susceptibility of the material  $\text{ZnCu}_3(\text{OH})_6\text{Cl}_2$  can be understood in terms of Dzyaloshinsky-Moriya anisotropies with  $D_p > |D_z|$ . We also show that the measured specific heat of the material puts further constraints on the allowed DM parameters.

PACS numbers: 75.10.Jm, 05.50.+q, 05.70.-a

## I. INTRODUCTION

The possible realization of exotic states of matter has always been at the forefront of research interest in condensed matter physics. One class of states, which has received considerable interest over the last few decades, consists of quantum spin liquids.<sup>1</sup> In these states, no magnetic order or other symmetry breaking occurs as the temperature is lowered, while the system may or may not exhibit a gap in its excitation spectra. Two variants of the quantum spin liquid have received particular attention recently: (i) a topological spin liquid, which has a spin gap and a topological order,<sup>2,3</sup> and (ii) an algebraic spin liquid, where there is no spin gap and spin-spin correlations decay as a power law.<sup>4,5</sup> Kagome lattice antiferromagnets are potential candidates for both these types of spin liquids.

Recently, the newly synthesized herbertsmithite<sup>6</sup>  $\text{ZnCu}_3(\text{OH})_6\text{Cl}_2$  has brought tremendous excitement to the field. For this rare mineral, in which the spin- $\frac{1}{2}$  copper atoms form a kagome lattice, like the one depicted in Fig. 1, no magnetic order is observed down to 50 mK (Refs. 7,8,9,10) even though the exchange constant is approximately 170 K.<sup>11</sup>

The spin- $\frac{1}{2}$  kagome lattice Heisenberg model (KLHM) has been extensively studied using series expansions and exact diagonalization of finite-size periodic clusters.<sup>12,13,14,15,16,17,18,19</sup> Exact diagonalization (ED) studies suggest that this model does not exhibit any magnetic order but possibly has a small spin gap  $\sim J/20$ . In addition, in finite systems, it has been found that there are a large number of singlet states below the spin gap and that their number grows with the system size,<sup>17,20</sup> which indicates that in the thermodynamic limit, non-magnetic excitations may develop a continuum beside the ground state.

Considering the above theoretical results, the experimental behavior of the recently synthesized kagome sys-

tems,  $\text{ZnCu}_3(\text{OH})_6\text{Cl}_2$ , is highly unexpected.<sup>7,8</sup> At high temperatures, the inverse susceptibility data was found to obey a Curie-Weiss law, with an effective Curie-Weiss constant of about 300 K. However, no spin gap was seen either in the susceptibility, the specific heat, the neutron spectra, or in the nuclear spin-lattice relaxation  $T_1$ , down to temperatures below 100 mK. In addition, at the lowest temperatures, the susceptibility saturates to very high values and the specific heat shows power-law behavior in temperature. The latter is suppressed by magnetic fields, showing it to be magnetic in origin.

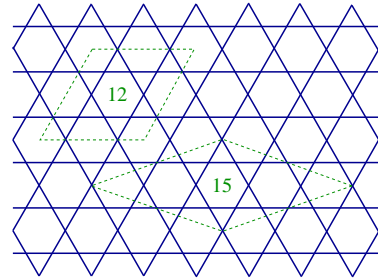


FIG. 1: (Color online) The kagome lattice. The embedded finite clusters are used (with periodic boundary conditions) in the ED study of DM interactions.

A possible interpretation of the substantial rise in the susceptibility seen experimentally at low temperatures is that it is due to impurity spins outside the kagome planes, possibly caused by substitutions of non magnetic Zn sites with Cu.<sup>21</sup> This idea has been reinforced in recent numerical analysis of Misguich and Sindzingre.<sup>22</sup> They find that the deviation of the experimental data from the kagome lattice Heisenberg model at least down to  $T \approx 40$  K can be understood in terms a small concentration of impurities provided the impurity contribution also has a weak ferromagnetic Curie-Weiss constant. We, on the other hand, have argued that the sharp rise in the susceptibility seen experimentally is intrinsic and it is related to the presence

of Dzyaloshinsky-Moriya (DM) interactions.<sup>11</sup> The latter is consistent with the experimental observation that the muon shift  $K$  tracks the bulk susceptibility  $\chi$ .

The two different explanations can be distinguished by studying single crystals, whereby the susceptibilities along different crystallographic axes can be investigated. The explanations based on DM interactions lead to substantial temperature dependent anisotropy in the susceptibility, whereas the impurity contributions should be isotropic. In the absence of single crystals, recent NMR work of Imai *et al.*<sup>10</sup> may already provide some resolution of the issue. Imai *et al.* find that the NMR spectra progressively broaden as one goes to lower temperatures. While the temperature dependence of the median of the broadened spectra resembles the sharp upturn seen in bulk susceptibility measurements, the spectra at the edges do not show this upturn. Rather, they show a saturation and eventually a downturn with lowering of temperature as expected in antiferromagnets, when short range order sets in. Indeed, we will see here that for certain choices of the DM parameters, susceptibilities along different crystallographic axes show the two different behaviors observed by Imai *et al.* Thus, one interpretation of the NMR experiments is that they are observing the susceptibility along different axes, due to the different alignment of the powders with respect to the applied field.

In this work, we further develop the DM theory by presenting a detailed study of the effects of in-plane ( $D_p$ ) and out-of-plane ( $D_z$ ) Dzyaloshinsky-Moriya interactions, as well as other perturbations such as easy-plane and easy-axis exchange anisotropies and quenched dilution, on the thermodynamic properties of the KLHM. We use ED and the triangle-based numerical linked cluster method (NLC)<sup>23</sup> to compute the uniform susceptibility, entropy, and specific heat. We find that unlike exchange anisotropy or dilution, the effects of DM interactions on the susceptibility can set in quite abruptly as a function of temperature. Furthermore, different choices of the DM parameters can lead to a wide range of behavior for the susceptibility. In particular, the abrupt upturn in the susceptibility seen experimentally in  $\text{ZnCu}_3(\text{OH})_6\text{Cl}_2$  around 75 K can be understood in terms of Dzyaloshinsky-Moriya anisotropies when  $D_p > |D_z|$ .

Also comparing the experimental specific heat data with their theoretical results, Misguich and Sindzingre<sup>22</sup> concluded that the measured entropy in the materials  $\text{ZnCu}_3(\text{OH})_6\text{Cl}_2$  at  $T/J = 0.06$  is much lower than for the pure KLHM, and that the very low temperature specific heat may be dominated by impurities. We discuss the role of DM interactions in the entropy and specific heat of the material. In general, DM interactions should lower the entropy as they reduce the manifold of classical ground states. We find that the entropy is reduced primarily due to  $D_z$ , whereas  $D_p$  has a very small effect on it. Thus, combining the experimental results on the susceptibility and specific heat, we believe that the most likely DM parameters for the material are in the range,

$D_p/J \approx 0.2 - 0.3$ ,  $|D_z|/J \approx 0.1$ . However, these results may change a little if impurity effects are included in the analysis.

The results of Misguich and Sindzingre<sup>22</sup> further substantiate our earlier assertion that the pure KLHM has an extended crossover regime,<sup>11</sup> where the susceptibility grows as a power law in inverse temperature and the specific heat or entropy is sublinear in temperature. From their numerical results, the power law in the susceptibility may extend over a full decade in temperature,  $0.1 < T/J < 1$ . We would like to reiterate that this crossover regime is important to address theoretically and may well be relevant to the properties of the real material.

This exposition is organized as follows. In Sec. II, we discuss the effects of Dzyaloshinsky-Moriya and exchange anisotropy on the susceptibility and compare them with experiments on  $\text{ZnCu}_3(\text{OH})_6\text{Cl}_2$ . In Sec. III, we study the consequences of the above mentioned perturbations and of quenched dilution on the entropy and specific heat and also discuss the constraints on the DM parameters for  $\text{ZnCu}_3(\text{OH})_6\text{Cl}_2$  that the specific heat (entropy) measurements introduce. Finally, the conclusions are presented in Sec. IV.

## II. UNIFORM SUSCEPTIBILITY

In this section, we study the effects of different perturbations on the uniform susceptibility of the spin- $\frac{1}{2}$  Heisenberg model. In a magnetic field  $\mathbf{h}$ , the Hamiltonian of this model can be written as

$$\mathcal{H} = J \sum_{\langle i,j \rangle} \mathbf{S}_i \mathbf{S}_j + \mathcal{H}_{pert} - g\mu_B \sum_i \mathbf{h} \cdot \mathbf{S}_i. \quad (1)$$

where  $J$  is the exchange coupling,  $g$  is the  $g$  factor (assumed to be isotropic),  $\mu_B$  is the Bohr magneton, and  $\mathcal{H}_{pert}$  represents the various perturbations. In what follows, we set  $J = 1$  and  $g\mu_B = 1$ . In the sum,  $\langle i, j \rangle$  means that only nearest neighbor interactions are considered.

The uniform susceptibility per spin is then given by

$$\chi_\alpha = \frac{T}{N} \left. \frac{\partial^2 \ln Z}{\partial h_\alpha^2} \right|_{\mathbf{h}=0}, \quad (2)$$

where  $Z$  is the partition function,  $T$  the temperature,  $N$  the number of lattice sites, and  $\alpha = x, y, z$ . The molar susceptibility  $\chi_{molar}$ , measured experimentally, is related to our susceptibility per spin by the relation  $\chi_{molar} = C\chi$ , where the constant  $C = N_A g^2 \mu_B^2 / kJ = 0.3752 \text{ g}^2/J$  in cgs units.

In a kagome lattice (which we assume lies in the  $x$ - $y$  plane), both out-of-plane ( $D_z$ ) and in-plane ( $D_p$ ) DM terms are allowed,<sup>24,25,26,27,28</sup>

$$\mathcal{H}_{DM} = \sum_{\langle i,j \rangle} D_z (\mathbf{S}_i \times \mathbf{S}_j)_z + \mathbf{D}_p \cdot (\mathbf{S}_i \times \mathbf{S}_j), \quad (3)$$

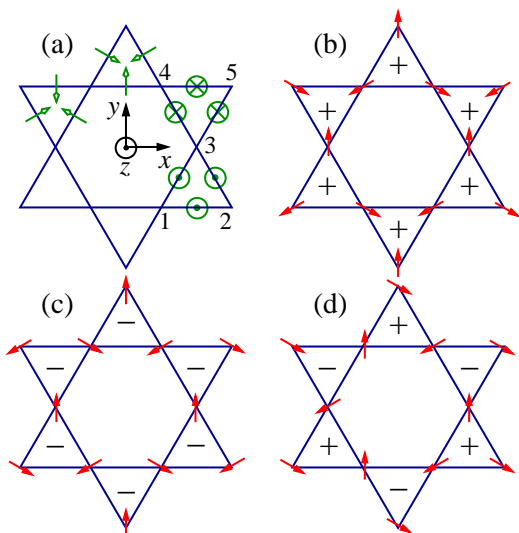


FIG. 2: (Color online) (a) Orientation of the in-plane and out-of-plane DM interactions. [(b)-(d)] Three possible classical ground states of the kagome lattice. In each case, the system has (b) positive chirality, (c) negative chirality, and (d) both positive and negative chiralities, as indicated by the signs inside the triangles.

Since the DM terms break spin rotational symmetry, we need to calculate separately the susceptibility with field along  $z$  ( $\chi_z$ ) and in the  $x$ - $y$  plane ( $\chi_p$ ). The powder susceptibility  $\chi_a$  is given by  $\chi_a = \frac{1}{3}(2\chi_p + \chi_z)$ .

With DM interactions, the different  $S^z$  sectors become coupled so that we are able to do NLC calculations only up to six triangles.<sup>23</sup> Unfortunately, the convergence of the KLHM with additional DM anisotropy is poor, and having only very few terms for the NLC expansion does not allow us to perform extrapolations. Hence, we turn to ED of clusters with 12 and 15 sites (Fig. 1), and periodic boundary conditions, to study the effects of DM interactions. In all our plots, we include both the results for 12 and 15 sites. The region where they agree gives an idea of the temperature range where finite-size effects are small and one can be confident of the ED results.

### A. $D_z \neq 0$ , $D_p = 0$

We first consider the case of a pure out-of-plane DM interaction ( $D_z \neq 0$ ,  $D_p = 0$ ). The sign of the  $D_z$  term alternates between the up- and down-pointing triangles of the kagome lattice. It can be set by demanding that for the up pointing triangle shown in Fig. 2 with corners 1-2-3, a positive  $D_z$  multiplies  $(\mathbf{S}_1 \times \mathbf{S}_2)_z$ , and for the down-pointing triangle 3-4-5, a negative  $D_z$  multiplies  $(\mathbf{S}_4 \times \mathbf{S}_5)_z$ .

The effect of a pure out-of-plane DM interaction is to favor the spins to lie in the  $x$ - $y$  plane. In that sense, it acts like an *easy-plane exchange anisotropy*. In addition, the sign of  $D_z$  breaks the chiral symmetry of the KLHM.

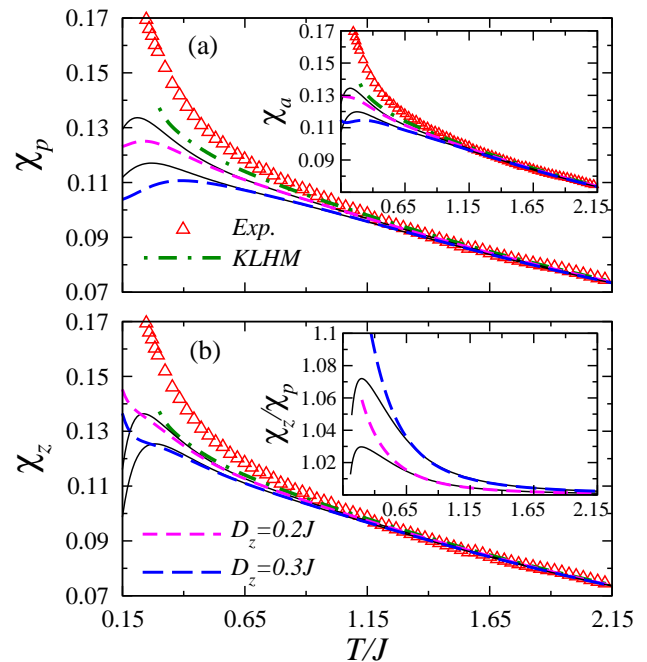


FIG. 3: (Color online) Temperature dependence of the (a) in-plane and (b) out-of-plane susceptibilities in the presence of a pure  $D_z$  anisotropy. They are compared with  $\chi$  for the pure KLHM [computed using the triangle based NLC expansion considering up to eight triangles (Ref. 23)] and with the experimental results (Refs. 7 and 8) translated to our notation (Ref. 29). In the inset in (a), we show the powder susceptibility and in the inset in (b) the anisotropy. In all plots of DM calculations, thick (thin) lines show the ED results of the 15 (12) site cluster.

In the classical limit, the ground state of the Heisenberg antiferromagnet is highly degenerate. All states satisfying the “120<sup>o</sup>” rule in each triangle minimize the energy. In Figs. 2(b)-2(d), we show three possible Néel states of the KLHM, where spins lie in the plane and which have positive, negative, and mixed chiralities, respectively. Once the  $z$  component of the DM interaction is introduced, the degeneracy between the states in Fig. 2 is lifted. For  $D_z > 0$ , the state with negative chirality [Fig. 2(c)] is favored, while for  $D_z < 0$ , the state with positive chirality [Fig. 2(b)] is the one that minimizes the energy.

Returning to our spin-half quantum model, in Fig. 3 we show the in-plane and out-of-plane susceptibilities as a function of temperature for two different strengths of  $D_z$ . (If only  $D_z$  is present, its sign is irrelevant for the thermodynamic quantities we study in this paper.) We compare these results with the ones obtained for the pure KLHM<sup>23</sup> and the ones measured experimentally for  $\text{ZnCu}_3(\text{OH})_6\text{Cl}_2$ .<sup>7,8</sup> Two features are apparent in these plots, which can be related to the increase of in-plane correlations between spins, as expected from classical considerations. (i) The  $D_z$  term suppresses both  $\chi_p$  and  $\chi_z$  with respect to the KLHM result and (ii)  $\chi_z$  becomes larger than  $\chi_p$ . Since the experimental result for the pow-

der susceptibility is larger than the one for the KLHM, it is evident [inset in Fig. 3(a)] that a  $D_z$  term alone cannot explain the experiments. The anisotropy produced by  $D_z$  in the susceptibilities is shown in the inset in Fig. 3(b).

There is another feature in the plots in Fig. 3 that is noticeable: finite-size effects set in at higher temperatures for  $\chi_p$  than for  $\chi_z$ . This confirms that the planar ( $XY$ ) correlations are longer ranged than the  $ZZ$  correlations.

### B. $D_p \neq 0, D_z = 0$

We now analyze an in-plane DM interaction  $D_p$ . It is perpendicular to the bonds and points inward toward the center of the triangles.<sup>27,28</sup> This is shown by the arrows in Fig. 2(a). (A different scenario for  $D_p$  is discussed in the Appendix.)  $D_p$  breaks the rotational symmetry around the  $c$  axis. It also favors classical spin configurations with a finite  $z$  component, producing weak ferromagnetism.<sup>26,27</sup> In that sense,  $D_p$  can act like an *easy-axis exchange anisotropy*.

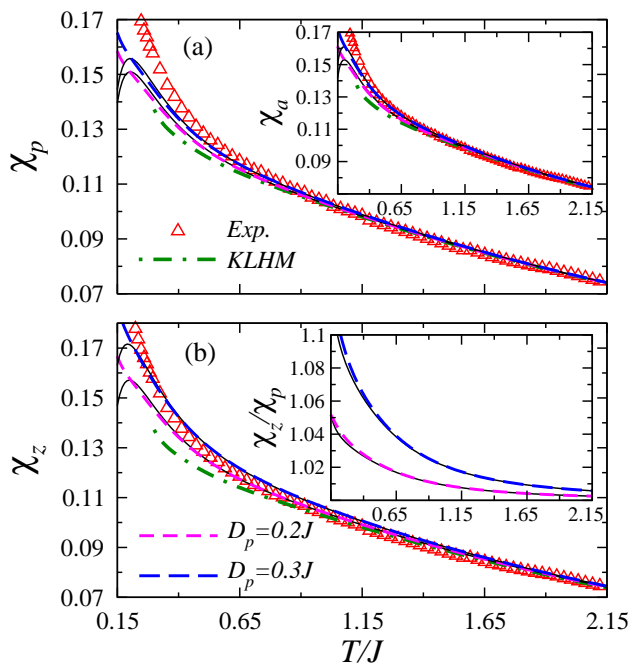


FIG. 4: (Color online) Temperature dependence of (a) the in-plane and (b) out-of-plane susceptibilities in the presence of a pure  $D_p$  anisotropy. They are compared with  $\chi$  for the pure KLHM (Ref. 23) and with the experimental results (Refs. 7 and 8). In the inset in (a), we show the powder susceptibility, and in the inset in (b) the anisotropy. In all plots of DM calculations, thick (thin) lines show the ED results of the 15 (12) site cluster.

In Fig. 4, we depict the  $x$ - $y$  and  $z$  susceptibilities as a function of the temperature for two different strengths of  $D_p$ .<sup>30</sup> As for  $D_z$ , we compare our results with the ones obtained for the pure KLHM<sup>23</sup> and the ones measured experimentally.<sup>7,8</sup> We find that a  $D_p$  term enhances both

$\chi_p$  and  $\chi_z$  with respect to the KLHM result, and that  $\chi_z$  becomes larger than  $\chi_p$ . This can be understood considering that  $D_p$ , when trying to produce canting, competes with the Heisenberg terms and reduces the in-plane spin-spin correlations.

The enhancement of  $\chi_p$  and  $\chi_z$  seen in Fig. 4 shows that a pure  $D_p$  term can explain the upturn seen experimentally for the susceptibility. This can be seen in the plots of the powder susceptibilities presented in the inset in Fig. 4(a). Interestingly, the anisotropies produced by  $D_z$  and  $D_p$  are very similar, as can be concluded by comparing the inset in Fig. 4(b) with the one in Fig. 3(b). They both generate  $\chi_z > \chi_p$ , and  $\chi_z/\chi_p$  are of the same order (at least for the intermediate temperatures studied here) when  $D_z$  and  $D_p$  are of the same order.

A remarkable difference between the effect of a  $D_z$  term and the effect of a  $D_p$  term in our finite cluster calculation of the susceptibilities is that in the latter, finite-size effects are very small as compared to the former one. This implies that all correlations are much weaker in the presence of a  $D_p$  term than in the presence of a  $D_z$  term.

### C. $D_p \neq 0, D_z \neq 0$ , and the experiments

Once  $D_p \neq 0$ , in general, thermodynamic quantities for  $D_z > 0$  start to differ from the ones for  $D_z < 0$ . In Fig. 5, we have plotted the in-plane and out-of-plane susceptibilities for a fixed value of  $D_p$  while increasing  $|D_z|$ , with  $D_z > 0$  [(a) and (b)] and  $D_z < 0$  [(c) and (d)]. Comparing Fig. 5(a) with Fig. 5(c) one can see that the increase of  $|D_z|$  produces the same effect in  $\chi_p$  no matter the sign of  $D_z$ . For both  $D_z > 0$  and  $D_z < 0$ , the in-plane susceptibility is suppressed with respect to its value for  $D_p \neq 0, D_z = 0$ . On the other hand, the effect produced by the increase of  $|D_z|$  on  $\chi_z$  is very different depending on the sign of  $D_z$ . Figure 5(b) shows that for  $D_z > 0$ , the increase of  $D_z$  suppresses  $\chi_z$  with respect to its value for  $D_p \neq 0, D_z = 0$ . As seen in Fig. 5(d), the opposite occurs if  $D_z < 0$ . The increase of  $|D_z|$  enhances  $\chi_z$  with respect to its value for  $D_p \neq 0, D_z = 0$ .

Given the above results for the in-plane and out-of-plane susceptibilities in the presence of  $D_p$  and  $D_z$ , one can then understand the behavior of the powder averages, which is presented in the insets of Figs. 5(a) and 5(b). For  $D_p \neq 0$  and  $D_z > 0$ , the increase of  $D_z$  monotonically reduces  $\chi_a$  from its value at  $D_z = 0$ . On the contrary, if  $D_p \neq 0$  and  $D_z < 0$ , a small increase of  $|D_z|$  enhances  $\chi_a$  at lower temperatures, producing a better agreement with the experiments than  $\chi_a$  for  $D_p \neq 0, D_z = 0$ . Ultimately, when  $|D_z| \sim D_p$ , the powder average of the susceptibility is again suppressed with respect to its value for  $D_z = 0$ .

Based on the results presented in Fig. 5, we conclude that the sharp upturn seen experimentally for the powder susceptibilities of the material  $\text{ZnCu}_3(\text{OH})_6\text{Cl}_2$  can be understood to be a consequence of DM interactions for  $D_p > |D_z|$  and  $D_z < 0$ . We predict that single crystal

measurements should see an upturn in the anisotropy when the powder susceptibility departs from the KLHM result. Such a behavior has also been seen for spin- $\frac{5}{2}$  kagome system  $\text{KFe}_3(\text{OH})_6(\text{SO}_4)_2$ .<sup>31</sup>

We should stress that in our theoretical calculations for the powder susceptibilities, we have assumed the  $g$  factor to be isotropic. As depicted in Fig. 5(d) for  $D_z < 0$ , the  $z$  susceptibility rises very rapidly, producing a large anisotropy  $\chi_z/\chi_p$  [shown in the inset in Fig. 5(d)]. Therefore, an expected anisotropic  $g$  factor enhanced along  $z$  will cause an even more rapid rise of  $\chi_a$  than the one presented in the inset in Fig. 5(b), and will lead to agreement with experiments with a smaller DM anisotropy. For example, already for  $D_p = 0.2J$  and  $|D_z| < D_p$ , the

$z$  susceptibility is very similar to the experimental result for the powder averages.

Another factor that could reduce the DM anisotropy required to describe the experimental results is the presence of a small concentration of impurity spins.<sup>21,22</sup> However, as this may vary from sample to sample, we will not consider it further in this work. As mentioned in the Introduction, even in the absence of single crystals, recent NMR work of Imai *et al.*<sup>10</sup> may support the relevance of DM interaction to  $\text{ZnCu}_3(\text{OH})_6\text{Cl}_2$ . The behavior they observe for the main peak and edges of the NMR spectra is similar to the powder [inset in Fig. 5(c)] or  $\chi_z$  [Fig. 5(d)] and in-plane [Fig. 5(c)] susceptibilities, respectively.

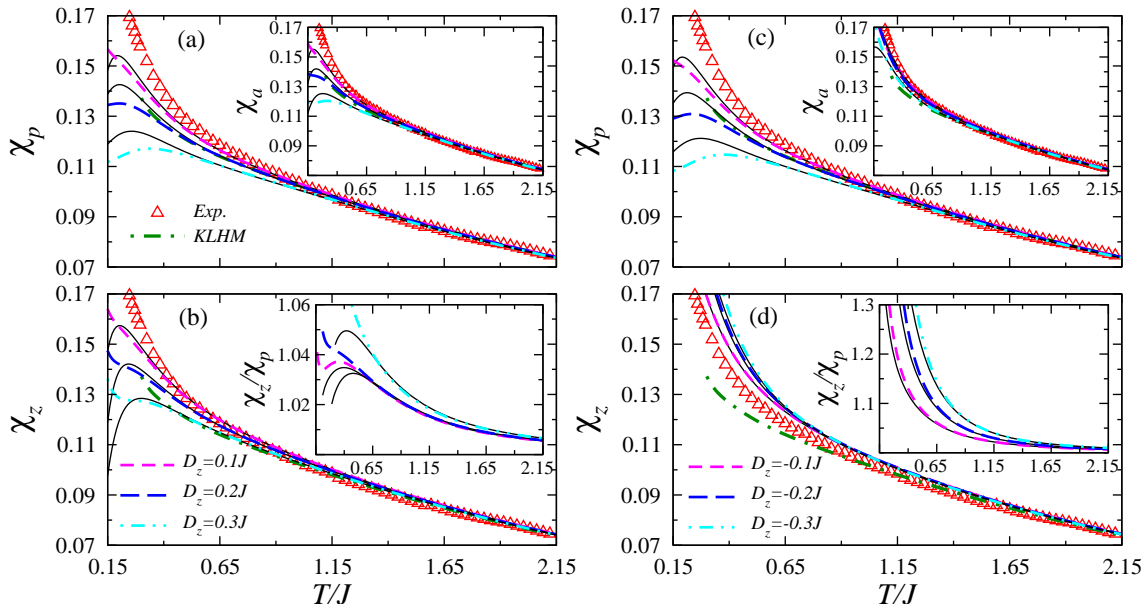


FIG. 5: (Color online) Temperature dependence of the [(a) and (c)] in-plane and [(b) and (d)] out-of-plane susceptibilities in the presence of an in-plane  $D_p = 0.3J$  anisotropy and different values and signs of the out-of-plane anisotropy. These susceptibilities are compared with  $\chi$  for the pure KLHM (Ref. 23) and with the experimental results (Refs. 7 and 8). In the inset in (a) and (c), we show powder susceptibilities, and in the inset in (b) and (d) the anisotropies. In all plots of DM calculations, thick (thin) lines show the ED results of the 15 (12) site cluster.

#### D. Exchange anisotropies

We discuss in what follows the role that exchange anisotropies play in the behavior of the magnetic susceptibilities. Easy-plane ( $\Delta > 0$ ) and easy-axis ( $\Delta < 0$ ) exchange anisotropies can be introduced perturbing the Heisenberg Hamiltonian with a term

$$\mathcal{H}_{EA} = \Delta \sum_{\langle i,j \rangle} (S_i^x S_j^x + S_i^y S_j^y). \quad (4)$$

Equation (4) breaks the  $\text{SU}(2)$  symmetry of the KLHM, however; it does not couple different  $S^z$  sectors. Hence, in the absence of  $x$ - $y$  magnetic fields, we can perform calculations for out-of-plane susceptibilities, entropy, and specific heat using the triangle-based NLC expansion summing contributions of up to eight triangles.

Calculating the in-plane susceptibilities [Eq. (2)] requires introducing  $x$ - $y$  magnetic fields, which couples different  $S^z$  sectors. Consequently, NLC calculations for  $\chi_p$  can be done only up to six triangles. As we will show later, in the presence of exchange anisotropies, NLC results for  $\chi_p$  are very similar to the ones obtained with ED (15 site cluster) down to  $T \sim 0.35J$ . For all other quantities, we only present NLC results, which are more accurate.

##### 1. Easy-plane exchange anisotropy

Figure 6 shows that an easy-plane exchange anisotropy decreases both the in-plane and out-of-plane susceptibilities with respect to the pure Heisenberg model, and  $\chi_z$  becomes larger than  $\chi_p$ , similar to the effect of a pure  $D_z$  term shown in Fig. 3. There are, however, clear dif-

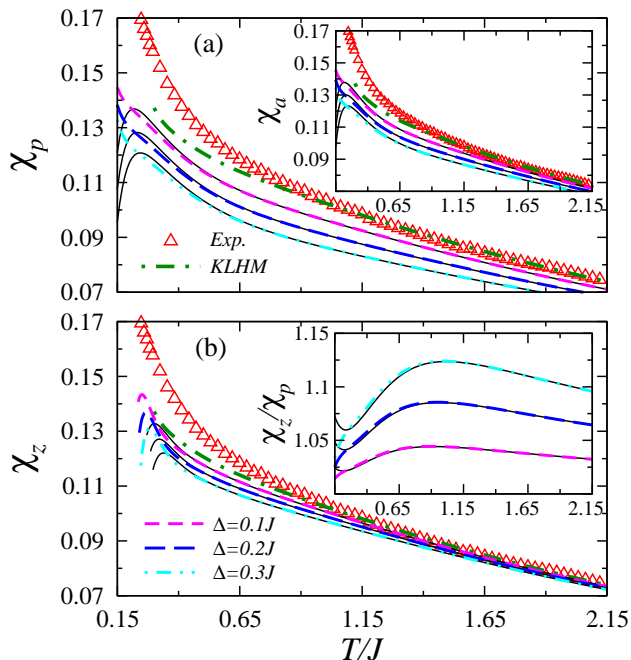


FIG. 6: (Color online) Temperature dependence of the (a) in-plane and (b) out-of-plane susceptibilities in the presence of an easy-plane exchange anisotropy. Results are compared with  $\chi$  for the pure KLHM (Ref. 23) and with the experimental results (Refs. 7 and 8). In the inset in (a), we show the powder susceptibility, and in the inset in (b) the anisotropy. In (a) and the insets of (a) and (b), the susceptibilities were computed using ED. Thick (thin) lines show the ED results of the 15 (12) site cluster. In (b), the  $z$  susceptibilities were obtained using NLC. Thick (thin) lines are the results of the NLC expansion with up to eight (seven) triangles.

ferences between  $\Delta > 0$  and  $D_z \neq 0$ . The easy-plane exchange anisotropy produces a large reduction of  $\chi_p$  [Fig. 6(a)] and  $\chi_a$  [inset in Fig. 6(a)] at high temperatures, and this reduction does not depend strongly on temperature down to  $T \sim 0.3J$ .

The above property of the exchange anisotropy highlights how remarkable DM interactions are. Their effect on the susceptibilities is negligible at high temperatures (even for large values of  $D_z$ ) and only onsets as the temperature is lowered. Another important difference between an easy-plane exchange anisotropy and the pure out-of-plane DM term is that, as shown in the inset in Fig. 6(b), the behavior of the anisotropy  $\chi_z/\chi_p$  produced by the former perturbation is nonmonotonic with temperature. Hence, susceptibility experiments with single crystals should be able to easily distinguish between these two types of anisotropies.

## 2. Easy-axis exchange anisotropy

The effect of an easy-axis exchange anisotropy on the susceptibility is depicted in Fig. 7. Like  $D_p$ ,  $\Delta < 0$  enhances both  $\chi_p$  and  $\chi_z$  with respect to  $\chi$  in the pure

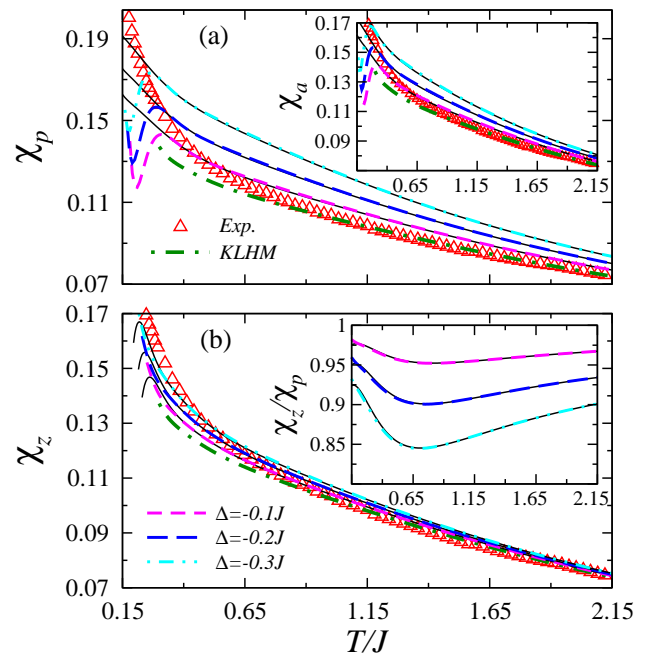


FIG. 7: (Color online) Temperature dependence of the (a) in-plane and (b) out-of-plane susceptibilities in the presence of an easy-axis exchange anisotropy. Results are compared with  $\chi$  for the pure KLHM (Ref. 23) and with the experimental results (Refs. 7 and 8). In the inset in (a), we show the powder susceptibility, and in the inset in (b) the anisotropy. In (a) and its inset, we compare results of the NLC expansion with up to six triangles (thick lines) with ED of a 15 site cluster (thin lines). In (b), the susceptibilities were obtained using the NLC expansion with up to eight triangles (thick lines) and seven triangles (thin lines). The anisotropies [inset in (b)] were obtained using ED of 15 site (thick lines) and 12 site (thin lines) clusters.

KLHM case. However,  $\Delta < 0$  has a large effect on  $\chi_p$  [Fig. 7(a)] and  $\chi_a$  [inset in Fig. 7(a)] at high temperatures. Basically,  $\Delta < 0$  produces a large enhancement of the susceptibility that is not strongly dependent on the temperature down to  $T \sim 0.3J$ .<sup>32</sup> Hence,  $\Delta < 0$  cannot provide an explanation for the sharp increase seen experimentally in the powder susceptibility. Notice also that in presence of an easy-axis exchange anisotropy, the in-plane susceptibilities are larger than the out-of-plane ones, and their anisotropy [inset in Fig. 7(b)] is nonmonotonic in temperature.

## III. ENTROPY AND SPECIFIC HEAT

In this section, we study the entropy ( $S$ ),

$$S = \frac{1}{N} (\ln Z + \langle \mathcal{H} \rangle / T), \quad (5)$$

and specific heat ( $C_v$ ),

$$C_v = \frac{1}{NT^2} (\langle \mathcal{H}^2 \rangle - \langle \mathcal{H} \rangle^2), \quad (6)$$

of the KLHM in the presence of various perturbations. In Eqs. (5) and (6),  $N$  stands for the number of lattice sites and  $Z$  for the partition function.

**A.  $D_z \neq 0$ ,  $D_p = 0$ , and  $\Delta > 0$**

We start by considering the effect of an out-of-plane DM anisotropy. Results for  $S$  and  $C_v$  and different values of  $D_z$  are shown in Fig. 8. As expected from the qualitative analysis in the previous section, where we argued that  $D_z$  breaks the degeneracy among different possible Néel states for KLHM, Fig. 8(a) shows that as the temperature is reduced,  $D_z$  reduces the entropy with respect to its value for the KLHM. This suppression of the entropy is accompanied by a large increase in the specific heat with respect to the KLHM. While for very small values of  $D_z$  a high-temperature peak can still be seen in  $C_v$  [Fig. 8(b)], by the time  $D_z = 0.3J$ , any evidence of such a peak has disappeared.

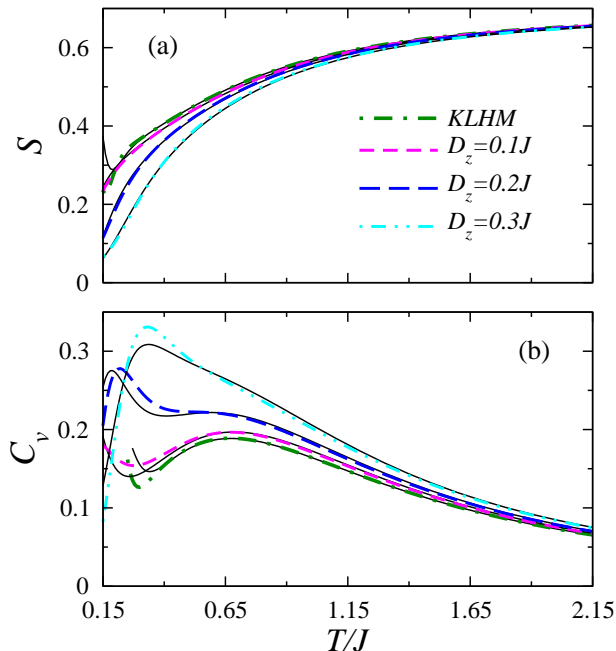


FIG. 8: (Color online) (a) Entropy and (b) specific heat as a function of the temperature in the presence of an out-of-plane DM interaction. For the KLHM, we used the NLC triangle-based expansion (Ref. 23) considering up to eight triangles (thick line) and seven triangles (thin line). For all plots with  $D_z \neq 0$ , thick (thin) lines show the ED results of the 15 (12) site cluster calculation.

As mentioned in Sec. II, the easy-plane exchange anisotropy [Eq. (4)] produces some features that are similar to a pure  $D_z$  term. In Fig. 9, we show the effects of  $\Delta > 0$  on  $S$  and  $C_v$ . Indeed, like  $D_z$ , an easy-plane anisotropy suppresses the entropy with respect to the KLHM. This reduction, however, is apparent at high temperatures even if  $\Delta$  is small, while in the presence

of  $D_z$  [Fig. 8(a)], it is only noticeable as the temperature is lowered.

The effect of  $\Delta > 0$  on the specific heat is very different from that of  $D_z$ , as seen in Fig. 9(b). Increasing  $\Delta$  (up to  $\Delta = 0.3J$ ) only displaces the high-temperature peak to higher temperatures almost without changing its height. (Eventually, as the exchange anisotropy is further increased toward the XY limit, the height of the  $C_v$  peak would decrease.) This means that if one could extract the behavior of  $S$  and  $C_v$  from experiments, one could further distinguish between DM and exchange anisotropies.

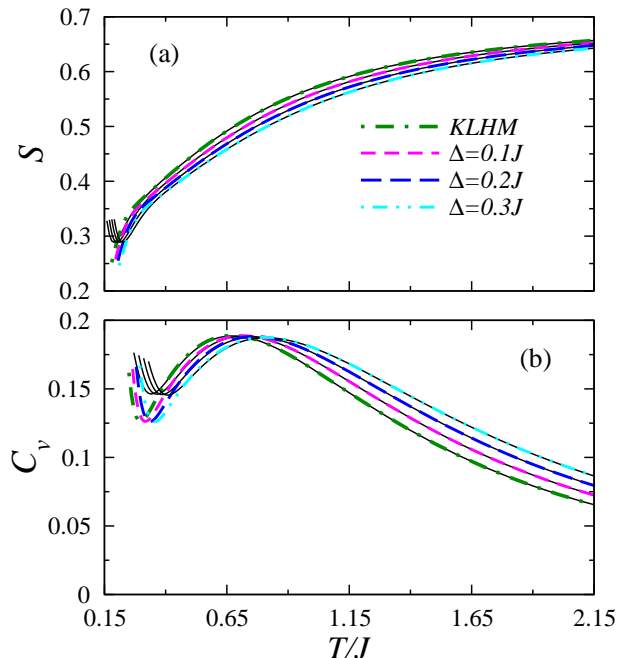


FIG. 9: (Color online) (a) Entropy and (b) specific heat as a function of the temperature in the presence of an easy-plane exchange anisotropy. All results were obtained using the NLC triangle-based expansion (Ref. 23) considering up to eight triangles (thick line) and seven triangles (thin line).

**B.  $D_p \neq 0$ ,  $D_z = 0$ , and  $\Delta < 0$**

We now turn to the effects of a pure in-plane DM anisotropy on the entropy and specific heat. This is depicted in Fig. 10. Figures 10(a) and 10(b) show that, at least down to temperatures  $\sim 0.15J$ ,  $D_p$  has a negligible effect on the entropy and specific heat, respectively. Considering that the largest  $D_p$  in Fig. 10 is 30% of  $J$  and that such anisotropy produces large changes in the uniform susceptibilities (Fig. 4), we find this feature remarkable.

We should add that as  $D_p$  is increased, the small displacement seen in the high temperature peak [Fig. 10(b)] toward higher temperatures is of the same order as the ED finite-size effects. To make that clear, we have also plotted  $D_p = 0$  results obtained from the exact diagonalization of a finite cluster with 15 sites. As better seen in

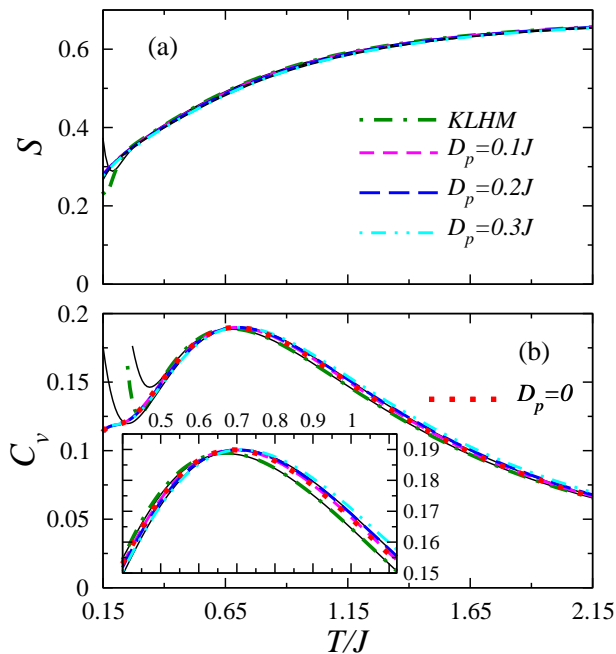


FIG. 10: (Color online) (a) Entropy and (b) specific heat as a function of the temperature in the presence of an in-plane DM interaction. For the KLHM, we used the NLC triangle-based expansion (Ref. 23) considering up to eight triangles (thick line) and seven triangles (thin line). For all plots with  $D_p \neq 0$ , thick (thin) lines show the ED results of the 15 (12) site cluster calculation. In (b), the extra plot denoted by  $D_p = 0$  is the KLHM ED result obtained with a 15 site cluster. The inset in (b) magnifies the high-temperature peak of  $C_v$  so that ED finite-size effects become discernible.

the inset, the ED peak for  $D_p = 0$  is slightly displaced toward higher temperatures than the thermodynamic limit result provided by NLC, and that displacement is of the same order as the one seen for  $D_p \neq 0$ . ( $C_v$  is, in general, very sensitive to finite-size effects.<sup>23</sup>)

The presence of an easy-axis exchange anisotropy has a very different effect on  $S$  and  $C_v$  of the KLHM. This can be seen by comparing Fig. 11 with Fig. 10. The increase of  $|\Delta|$  increases the entropy, at all temperatures, with respect to the KLHM. This is expected since in the Ising limit, the system has a finite entropy at zero temperature. For  $C_v$ , what happens is that the high-temperature peak moves to lower temperatures. The height of the peak almost does not change up to  $\Delta = -0.3J$ , although it eventually decreases as  $\Delta$  approaches -1.<sup>23</sup>

### C. $D_p \neq 0$ , $D_z \neq 0$

If both DM terms are present in the system, we find that the deviations of  $S$  and  $C_v$  from the KLHM result (in the range of temperatures discussed in this work) are mainly determined by the value of  $D_z$ , almost independent of the value (and sign) of  $D_p$  (up to  $D_p \sim 0.3J$ ). Hence, at least at intermediate and high

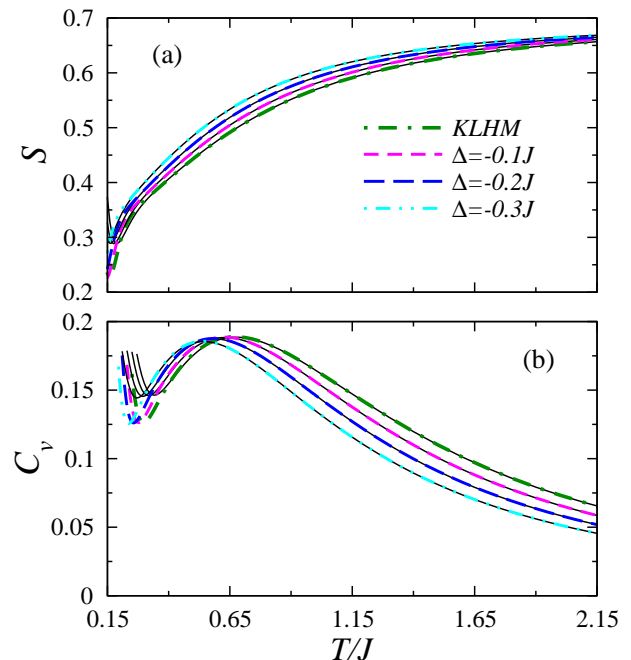


FIG. 11: (Color online) (a) Entropy and (b) specific heat as a function of the temperature in the presence of an easy-axis exchange anisotropy. All results were obtained using the NLC triangle-based expansion (Ref. 23) considering up to eight triangles (thick line) and seven triangles (thin line).

temperatures,  $S$  and  $C_v$  are quite insensitive to the existence of an in-plane DM interaction. This is further discussed in a later section in comparison to experiments on  $\text{ZnCu}_3(\text{OH})_6\text{Cl}_2$ .

### D. Quenched dilution

As discussed in Ref. 11, another important perturbation of the KLHM is the presence of quenched dilution. Quenched dilution could be generated in the materials  $\text{ZnCu}_3(\text{OH})_6\text{Cl}_2$  due to the substitution of Cu sites in the kagome planes by Zn. The missing spins on the lattice could create local moments in the singlet background and cause a Curie-like susceptibility to arise as the temperature is lowered. However, we have shown that at least down to temperatures  $T \sim 0.3J$ , the only effect that such a dilution has on the susceptibility is to suppress it with respect to the KLHM result.<sup>11</sup> In this sense, quenched dilution has the opposite effect of impurity spins as the latter enhance the susceptibility.

Here, we present studies of the effects of quenched dilution on entropy and specific heat of KLHM. Our calculations are performed using the triangle-based NLC expansion considering up to eight triangles. If  $c$  is the dilution, we assume that at each site we have a hole with probability  $c$  and a spin with probability  $1 - c$ . The holes are fixed in their position and extensive quantities are aver-



aged over all possible configurations  $C$  using the relation

$$\langle O \rangle = \sum_C P(C) O(C), \quad (7)$$

where

$$P(C) = c^{N_h} (1-c)^{N_s} \quad (8)$$

is the probability of the configuration  $C$  with  $N_h$  holes and  $N_s$  spins.

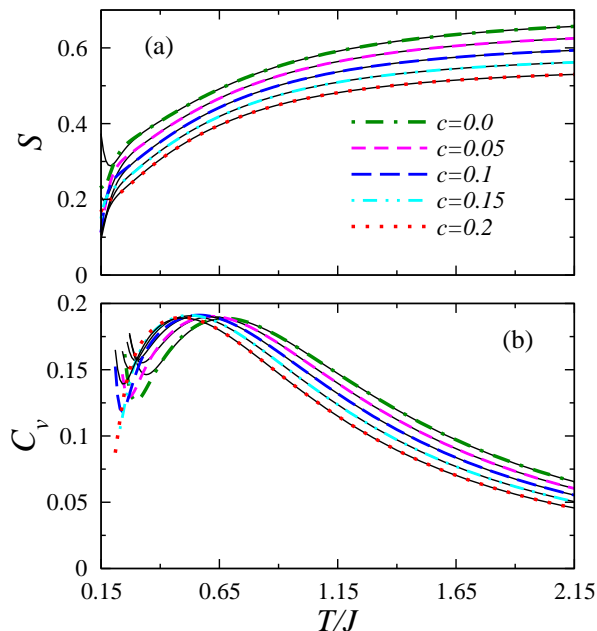


FIG. 12: (Color online) (a) Entropy and (b) specific heat as a function of the temperature in the presence of quenched dilution. All results were obtained using the NLC triangle-based expansion (Ref. 23) considering up to eight triangles (thick line) and seven triangles (thin line).

The entropy and specific heat for several values of hole concentration are shown in Fig. 12. We note that at these intermediate temperatures [Fig. 12(a)], holes simply lower the entropy at all temperatures. In the case of the specific heat, they just displace the high temperature peak to lower temperatures, almost without changing its height.

#### E. Entropy difference from kagome lattice Heisenberg model and implication for $\text{ZnCu}_3(\text{OH})_6\text{Cl}_2$

To conclude the section on specific heat and entropy, we study the entropy difference between the KLHM and the model with different DM parameters. Shown in Fig. 13 is  $\Delta S$ , given by

$$\Delta S = S(D_p = 0, D_z = 0) - S(D_p, D_z).$$

It is the reduction in entropy due to DM interactions. In Fig. 13, one notices that the entropy reduction is determined primarily by  $D_z$  and  $D_p$  plays a small role.

The diamond in Fig. 13 represents the minimum discrepancy between the pure KLHM and  $\text{ZnCu}_3(\text{OH})_6\text{Cl}_2$  at  $T/J = 0.06$  as determined by Misguich and Sindzingre (MS) in Ref. 22. The experimental data at higher temperatures are likely dominated by phonons. From Fig. 13, we conclude that  $|D_z|/J$  is likely to be about 0.1 in  $\text{ZnCu}_3(\text{OH})_6\text{Cl}_2$ . Hence, while the sharp increase in the susceptibility discussed in Sec. II allows us to make an estimate of the possible values of  $D_p$  ( $D_p/J \approx 0.2 - 0.3$ ), the entropy reduction allows us to get an estimate of  $|D_z|$ .

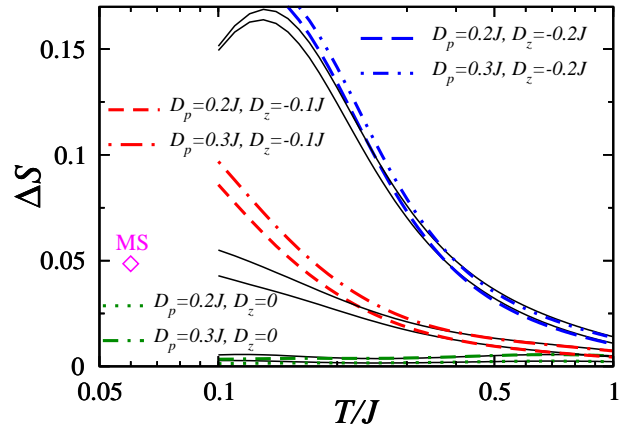


FIG. 13: (Color online) Difference between the entropy of the pure KLHM and the entropy of the KLHM in the presence of DM anisotropies. Thick dashed lines show the ED results of the 15 site cluster and the thin black lines result of 12 site cluster. The diamond at  $T = 0.06J$  depicts the minimum difference between the pure KLHM and the experimental result as obtained by MS in Ref. 22.

## IV. CONCLUSIONS

In this work, we have studied in detail the effect of perturbations such as in-plane and out-of-plane DM interactions, exchange anisotropies, and quenched dilution on the KLHM. We have focused here on the effect such perturbations have on magnetic susceptibilities, entropy, and specific heat. We first summarize our theoretical findings:

(i) In the presence of a pure out-of-plane DM term ( $D_z \neq 0$ ,  $D_p = 0$ ) both in-plane ( $\chi_p$ ) and out-of-plane ( $\chi_z$ ) susceptibilities are suppressed with respect to the KLHM result, and  $\chi_z$  becomes larger than  $\chi_p$ . However, the susceptibility anisotropy  $\chi_z/\chi_p$  is not large ( $< 1.1$ ) down to  $T \sim 0.5J$  for  $D_z \lesssim 0.3J$ . On the other hand, a  $D_z$  term suppresses the entropy as the temperature is lowered and produces an increase of the specific heat at intermediate temperatures.

(ii) In the presence of a pure in-plane DM term ( $D_z = 0$ ,  $D_p \neq 0$ ), both in-plane ( $\chi_p$ ) and out-of-plane ( $\chi_z$ )

susceptibilities are enhanced with respect to the KLHM result and, as for pure  $D_z$ ,  $\chi_z$  becomes larger than  $\chi_p$ . The susceptibility anisotropy is not large ( $< 1.1$ ) down to  $T \sim 0.25J$  for  $D_p \lesssim 0.3J$ . A  $D_p$  term ( $\lesssim 0.3J$ ) has a negligible influence on entropy and specific heat down to  $T \sim 0.15J$ .

(iii) When both  $D_p$  and  $D_z$  are present, the susceptibility becomes sensitive to the sign of  $D_z$ . (A) For a constant value of  $D_p$ , the increase of  $D_z$  for  $D_z > 0$  suppresses both the in-plane and out-of-plane susceptibilities with respect to the  $D_z = 0$  value. The susceptibility anisotropy is of the same order as when only  $D_p$  or  $D_z$  is present. (B) Also keeping  $D_p$  constant, the increase of  $|D_z|$  for  $D_z < 0$  suppresses the in-plane susceptibility but enhances the out-of-plane susceptibility.

(iv) In the presence of both  $D_p$  and  $D_z$ , the entropy and specific heat are mainly determined by the modulus of  $D_z$ .  $D_p$  and the sign of  $D_z$  play a relatively small role.

(v) The presence of an easy-plane exchange anisotropy suppresses both  $\chi_p$  and  $\chi_z$  from their KLHM values, and  $\chi_z$  becomes larger than  $\chi_p$ . Such anisotropy has a large effect even at high temperatures and does not produce deviations from the KLHM that are strongly temperature dependent. In addition, it generates susceptibility anisotropies that are nonmonotonic and weakly dependent on temperature down to  $T \sim 0.25J$ .  $\Delta > 0$  also suppresses the entropy with respect to the KLHM. The high-temperature peak of the specific heat is slightly displaced toward higher temperatures almost without modifying its height (for  $\Delta \lesssim 0.3J$ ).

(vi) The presence of an easy-axis exchange anisotropy enhances both  $\chi_p$  and  $\chi_z$  from their KLHM values, and  $\chi_p$  becomes larger than  $\chi_z$ .  $\Delta < 0$  has a large effect on the high-temperature values of  $\chi_p$  and also does not produce deviations from the KLHM that are strongly temperature dependent. It also leads to susceptibility anisotropies that are nonmonotonic and weakly dependent on the temperature down to  $T \sim 0.25J$ .  $\Delta < 0$  also enhances the entropy with respect to the KLHM result. The high-temperature peak of the specific heat is slightly displaced toward lower temperatures without much change in height (for  $|\Delta| \lesssim 0.3J$ ).

(vii) At intermediate and high temperatures ( $T \gtrsim 0.3J$ ), quenched dilution has been shown to suppress the uniform susceptibility with respect to the KLHM.<sup>11</sup> We have discussed here that it also reduces the entropy for all temperatures  $T \gtrsim 0.3J$ . In the case of the specific heat, the effect of dilution is to displace the high temperature peak toward lower temperatures without affecting its height (at least when  $c \lesssim 0.2$ ).

We now discuss our conclusions with regard to the observed properties of the material  $\text{ZnCu}_3(\text{OH})_6\text{Cl}_2$ :

(i) The observed susceptibility shows large enhancement with respect to the KLHM, which has a sudden onset below  $T = J/2$ . This kind of behavior is only compatible, within the models studied, with a large  $D_p \approx 0.2 - 0.3$  and a  $D_z < 0$ , with  $|D_z| < D_p$ .

(ii) Misguich and Sindzingre<sup>22</sup> have previously con-

cluded that the experiments on  $\text{ZnCu}_3(\text{OH})_6\text{Cl}_2$  show that there is a large reduction in entropy with respect to KLHM at  $T/J = 0.06$ . This reduction is at least 0.05 and may be larger when impurities and phonons are taken into account. The comparison with DM anisotropy calculations shows that this implies  $|D_z|/J \approx 0.1$ .

Based on these results, our overall conclusion for the parameters of the material  $\text{ZnCu}_3(\text{OH})_6\text{Cl}_2$  is  $D_p/J$  in the range  $0.20 - 0.30$ ,  $|D_z|/J \approx 0.1$ , and  $J \approx 170K$ . All these numbers could change if there are substantial impurity contributions present. Future experiments on the effects of anisotropy can resolve these issues.

On the theoretical side, an important question that remains open is the nature of the low-temperature phase(s) of the KLHM in the presence of DM terms. In classical systems, it has been shown that ground state is ordered,<sup>26,27</sup> and there is a finite temperature phase transition in which the critical temperature depends on the values of  $D_z$  and  $D_p$ .<sup>26</sup> However, one should keep in mind that for classical systems, even in the absence of DM anisotropy, the system orders as  $T$  goes to zero.<sup>34,35</sup> Quantum effects for the spin- $\frac{1}{2}$  case, and their relation to the experimental absence of any order down to 50 mK, still need to be elucidated.

## Acknowledgments

This work was supported by the US National Science Foundation, Grants Nos. DMR-0240918, DMR-0312261, and PHY-0301052. We are grateful to Oren Ofer, Amit Keren, Joel Helton, and Young Lee for providing us with the experimental susceptibility data, and to Michael Hermele and Takashi Imai for valuable discussions. We thank the HPCC-USC center where all our computations have been performed.

*Note added on proof.* –It has been argued in recent experiments<sup>36,37,38</sup> that contrary to the original expectation a rather large concentration of intersite mixing (Cu/Zn) impurities ( $c_s \sim 6 - 10\%$ ) may be present in the Herbertsmithite material. One natural question that has not been addressed in these works is whether such a large impurity concentration can be accommodated to reproduce the intermediate and high temperature magnetic susceptibility of the KLHM. In Ref. 11 we have shown that subtracting the contribution of  $c_s = 4.5\%$  free impurity spins ( $J = 200$  K) to the experimental results of Refs. 7 and 8 one can reproduce the magnetic susceptibility of the KLHM down to  $T = 0.3J$ . (The free impurity spin concentration reported in Ref. 11 was incorrect by a factor 3/2, which means that in Fig. 2 of that reference one should read  $c = 0.045$  and  $c = 0.09$  instead of  $c = 0.03$  and  $c = 0.06$ , respectively.) However, a sharp rise in the susceptibility remained below  $T = 0.3J$  that was not expected in the KLHM. It was shown later by Misguich and Sindzingre<sup>22</sup> that adding a small ferromagnetic coupling between impurities ( $c_s = 3.7\%$  and

$J = 190$  K) allows one to reproduce the magnetic susceptibility of the KLHM down to  $T = 0.2J$ , with  $\chi$  starting to decrease when  $T \sim 0.1J$ .

From the theoretical results in Refs. 11 and 22 one could conclude that after subtracting the large contribution of  $c_s \sim 6 - 10\%$  impurity spins (Cu) to the experimental results one would obtain a magnetic susceptibility that is incompatible with the KLHM at intermediate and high temperatures. However, such a large concentration of impurity spins can be accommodated if one considers the effect of the non-magnetic impurity counterpart (Zn) that is present in the kagome planes. As shown in Ref. 11 such impurities reduce the magnetic susceptibility with respect to the KLHM. Figure 14 shows that after subtracting a  $c_s \sim 6\%$  free impurity spin contribution from the experimental results one can reproduce the susceptibility of the KLHM with a  $c = 6\%$  of quenched nonmagnetic impurities.

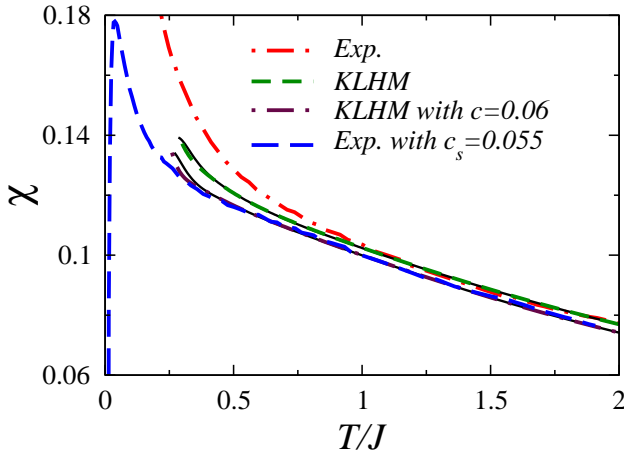


FIG. 14: (Color online) NLC results for the KLHM with ( $c = 6\%$ ) and without ( $c = 0$ ) nonmagnetic impurities are compared with the experimental results after a  $c_s = 5.5\%$  and  $c_s = 0$  contribution of free impurity spins is subtracted, i.e., in the latter case we have plotted  $\chi_{molar}/C - c_s/(4T)$  (where  $C$  was defined in Sec. II). In the presence of impurities we obtain  $J = 210$  K,  $g = 2.37$  as opposed to  $J = 170$  K,  $g = 2.33$  in their absence. NLC results for the eight(seven) triangle based expansion are plotted as thick(thin) lines.

The results presented in Fig. 14 show that a large concentration of intersite mixing (Cu/Zn) impurities is compatible with the KLHM at intermediate and high temperatures. However, whether impurities are the main contribution to the magnetic susceptibility at intermediate and low temperatures, as opposed to DM interactions, still needs to be clarified measuring the anisotropy in the in-plane and out-of-plane susceptibilities for temperatures where  $\chi$  clearly departs from the pure KLHM result.

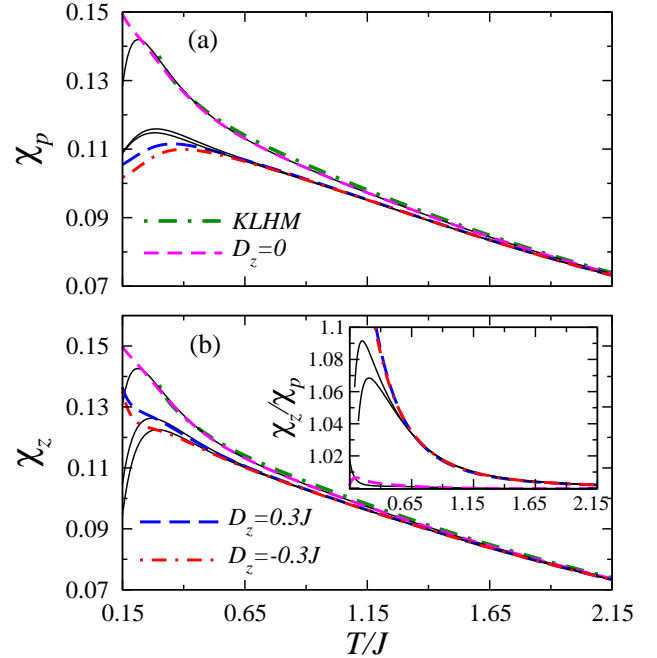


FIG. 15: (Color online) Temperature dependence of the (a) in-plane and (b) out-of-plane susceptibilities in the presence of a  $D_p = 0.3J$  anisotropy (with  $\mathbf{D}_p$  alternating from triangle to triangle as explained in the text) and different values of  $D_z$ . The results are compared with  $\chi$  for the pure KLHM (Ref. 23) In the inset in (b), we show the anisotropy produced by these DM terms. In all plots of DM calculations, thick (thin) lines show the ED results of the 15 (12) site cluster.

## APPENDIX A: DZYALOSHINSKY-MORIYA INTERACTIONS UNDER A DIFFERENT LATTICE SYMMETRY

In Sec. II, we discuss the effects of the DM anisotropy allowed by the symmetry of  $\text{ZnCu}_3(\text{OH})_6\text{Cl}_2$  on the susceptibility of the KLHM. In  $\text{ZnCu}_3(\text{OH})_6\text{Cl}_2$ , the bonds between  $\text{Cu}^{2+}$  ions (which have an oxygen atom in the middle) are distorted away from the kagome planes, and the direction of this distortion alternates from triangle to triangle. This symmetry of  $\text{ZnCu}_3(\text{OH})_6\text{Cl}_2$  sets the direction of  $\mathbf{D}_p$ , which within our notation is to be always pointing toward the center of the triangles.<sup>26,27</sup> [In Fig. 3, the  $\mathbf{D}_p$  that multiplies  $(\mathbf{S}_1 \times \mathbf{S}_2)_y$  is  $(0, D_p, 0)$ , and the one that multiplies  $(\mathbf{S}_4 \times \mathbf{S}_5)_y$  is  $(0, -D_p, 0)$ .] If the bonds between the Cu sites would not be distorted at all, a perfect kagome lattice would be embedded in three dimensions, because of the symmetry of the lattice  $\mathbf{D}_p = 0$ , and only  $D_z$  could be different from zero.<sup>24,25</sup>

For completeness, we briefly discuss here how the susceptibility of the KLHM would behave in a material where the bonds between magnetic ions are all distorted in the same direction away from the kagome planes. In this case, the  $D_z$  terms in Eq. (3) are identical to the ones we have considered for  $\text{ZnCu}_3(\text{OH})_6\text{Cl}_2$ , but the  $\mathbf{D}_p$  vectors will, within our notation, alternate pointing inward and outward of the up-pointing and down-pointing

triangles, respectively. That scenario seems to be very interesting within the discussion in Ref. 21.<sup>33</sup>

In Fig. 15, we depict the  $x$ - $y$  and  $z$  susceptibilities as a function of the temperature for  $D_p = 0.3J$  and three different values of  $D_z$ . One can see in Fig. 15 that, for  $D_z = 0$ , the kind of  $D_p$  anisotropy discussed in this appendix has almost no effect on the susceptibility of the KLHM, at least for the temperatures considered in this work. The inset in (b) shows that it also does not generate any asymmetry between  $\chi_p$  and  $\chi_z$ . Introducing a finite  $D_z$ , either positive or negative, only suppresses

(in a very similar way independent of the sign) both in-plane and out-of-plane susceptibilities with respect to the KLHM. (Similar to the discussion in Sec. III, the  $D_p$  anisotropy discussed in this appendix is almost irrelevant to the entropy and specific heat.)

Hence, in kagome lattice materials with a crystal symmetry different from that of  $\text{ZnCu}_3(\text{OH})_6\text{Cl}_2$ ,  $D_p$  anisotropies will produce a very different behavior of the susceptibility, which will not be enhanced with respect to the one of the KLHM.

- 
- <sup>1</sup> P. W. Anderson, Mater. Res. Bull. **8**, 153 (1973).  
<sup>2</sup> S. A. Kivelson, D. S. Rokhsar, and J. P. Sethna, Phys. Rev. B **35**, 8865 (1987).  
<sup>3</sup> R. Moessner and S. L. Sondhi, Phys. Rev. Lett. **86**, 1881 (2001).  
<sup>4</sup> M. B. Hastings, Phys. Rev. B **63**, 014413 (2001).  
<sup>5</sup> M. Hermele, T. Senthil, and M. P. A. Fisher, Phys. Rev. B **72**, 104404 (2005).  
<sup>6</sup> M. P. Shores, E. A. Nytko, B. M. Bartlett, and D. G. Nocera, J. Am. Chem. Soc. **127**, 13462 (2005).  
<sup>7</sup> J. S. Helton, K. Matan, M. P. Shores, E. A. Nytko, B. M. Bartlett, Y. Yoshida, Y. Takano, A. Suslov, Y. Qiu, J.-H. Chung, D. G. Nocera, and Y. S. Lee, Phys. Rev. Lett. **98**, 107204 (2007).  
<sup>8</sup> O. Ofer, A. Keren, E. A. Nytko, M. P. Shores, B. M. Bartlett, D. G. Nocera, C. Baines, and A. Amato, arXiv:cond-mat/0610540.  
<sup>9</sup> P. Mendels, F. Bert, M. A. de Vries, A. Olariu, A. Harrison, F. Duc, J. C. Trombe, J. Lord, A. Amato, and C. Baines, Phys. Rev. Lett. **98**, 077204 (2007).  
<sup>10</sup> T. Imai, E. A. Nytko, B. M. Bartlett, M. P. Shores, and D. G. Nocera, arXiv:cond-mat/0703141.  
<sup>11</sup> M. Rigol and R. R. P. Singh, Phys. Rev. Lett. **98**, 207204 (2007).  
<sup>12</sup> C. Zeng and V. Elser, Phys. Rev. B **42**, 8436 (1990).  
<sup>13</sup> R. R. P. Singh and D. A. Huse, Phys. Rev. Lett. **68**, 1766 (1992).  
<sup>14</sup> P. W. Leung and V. Elser, Phys. Rev. B **47**, 5459 (1993).  
<sup>15</sup> N. Elstner and A. P. Young, Phys. Rev. B **50**, 6871 (1994).  
<sup>16</sup> P. Lecheminant, B. Bernu, C. Lhuillier, L. Pierre, and P. Sindzingre, Phys. Rev. B **56**, 2521 (1997).  
<sup>17</sup> Ch. Waldtmann, H.-U. Everts, B. Bernu, C. Lhuillier, P. Sindzingre, P. Lecheminant, and L. Pierre, Eur. Phys. J. B **2**, 501 (1998).  
<sup>18</sup> P. Sindzingre, G. Misguich, C. Lhuillier, B. Bernu, L. Pierre, Ch. Waldtmann, and H.-U. Everts, Phys. Rev. Lett. **84**, 2953 (2000).  
<sup>19</sup> G. Misguich and B. Bernu, Phys. Rev. B **71**, 014417 (2005).  
<sup>20</sup> F. Mila, Phys. Rev. Lett. **81**, 2356 (1998).  
<sup>21</sup> Y. Ran, M. Hermele, P. A. Lee, and X.-G. Wen, Phys. Rev. Lett. **98**, 117205 (2007).  
<sup>22</sup> G. Misguich and P. Sindzingre, arXiv:0704.1017.  
<sup>23</sup> M. Rigol, T. Bryant, and R. R. P. Singh, Phys. Rev. Lett. **97**, 187202 (2006); Phys. Rev. E **75**, 061118 (2007).  
<sup>24</sup> I. E. Dzyaloshinsky, J. Phys. Chem. Solids **4**, 241 (1958).  
<sup>25</sup> T. Moriya, Phys. Rev. **120**, 91 (1960).  
<sup>26</sup> M. Elhajal, B. Canals, and C. Lacroix, Phys. Rev. B **66**, 014422 (2002).  
<sup>27</sup> T. Yildirim and A. B. Harris, Phys. Rev. B **73**, 214446 (2006).  
<sup>28</sup> Y. Yamabe, T. Ono, T. Suto, and H. Tanaka, arXiv:cond-mat/0607440.  
<sup>29</sup> For both experimental cases, we have taken  $J = 170$  K. The  $g$  factors needed for the fit are 2.33 for the data from Ref. 7 and 2.19 for the data from Ref. 8.  
<sup>30</sup> Thermodynamic quantities studied in this work are unaffected by the sign of  $D_p$ . We assume it to be positive without losing generality.  
<sup>31</sup> D. Grohol, K. Matan, J.-H. Cho, S.-H. Lee, J. W. Lynn, D. G. Nocera, and Y. S. Lee, Nat. Mater. **4**, 323 (2005).  
<sup>32</sup> Notice that the NLC results for  $\chi_p$  and  $\chi_a$  up to six triangles are almost indistinguishable from the ED result of a 15 site cluster down to  $T \sim 0.35J$ .  
<sup>33</sup> M. Hermele (private communication).  
<sup>34</sup> D. A. Huse and A. D. Rutenberg, Phys. Rev. B **45**, 7536 (1992).  
<sup>35</sup> J. N. Reimers and A. J. Berlinsky, Phys. Rev. B **48**, 9539 (1993).  
<sup>36</sup> M. A. de Vries, K. V. Kamenev, W. A. Kockelmann, J. Sanchez-Benitez, and A. Harrison, arXiv:0705.0654 (2007).  
<sup>37</sup> S.-H. Lee, H. Kikuchi, Y. Qiu, B. Lake, Q. Huang, K. Habicht, and K. Kiefer, Nature Mater. doi:10.1038/nmat1986 (2007).  
<sup>38</sup> F. Bert, S. Nakamae, F. Ladieu, D. L'Hôte, P. Bonville, F. Duc, J.-C. Trombe, and P. Mendels, arXiv:0710.0451 (2007).